Mechanical Systems and Signal Processing 116 (2019) 310–321

Contents lists available at ScienceDirect

Mechanical Systems and Signal Processing

journal homepage: www.elsevier.com/locate/ymssp

Combination of input shaping and radial spring-damper to reduce tridirectional vibration of crane payload

Viet Duc La [a,b,*], Kien Trong Nguyen [b,c]

[a] Institute of Mechanics, Vietnam Academy of Science and Technology, 264 Doi Can, Hanoi, Viet Nam
[b] Graduate University of Science and Technology, Vietnam Academy of Science and Technology, 18 Hoang Quoc Viet, Hanoi, Viet Nam
[c] Vinh University, 182 Le Duan Str., Vinh City, Nghe An, Viet Nam

ARTICLE INFO

Article history:
Received 5 March 2018
Received in revised form 26 May 2018
Accepted 28 June 2018

Keywords:
Coriolis damping
Crane swing control
Input shaping
Nonlinear damping
Spherical pendulum

ABSTRACT

The input shaping technique alters the human-operator commands to reduce the payload oscillation. A single radial spring-damper can simultaneously produce three dampings to suppress the tridirectional vibration of a crane payload. Combination of input shaping and radial spring-damper can be a sensorless approach to reduce the vibration induced by both operator commands and external disturbances. A numerical simulation of a boom crane is carried out to clarify the effectiveness of each component in the combination. An experiment of a laboratory boom crane is presented to show the effect of radial spring-damper.

1. Introduction

Cranes occupies a crucial role within industry. The improvement of cranes operational effectiveness can be extremely valuable. However, the payload suspended by cables is highly flexible in nature. Payload oscillation induced by motions of the support unit or external disturbances, such as wind is a major limitation.

The techniques proposed for anti-swing crane control include feedforward and feedback control. The feedback techniques generate the control command based on the crane measurements [1–7]. The fuzzy control [8], adaptive control [9], and predictive control [10] have been studied for the crane with parametric uncertainties and external disturbances. However, because almost all the cranes are operated by human, the feedback technique can causes the fundamental conflict between human and computer. To reduce the payload swing, the input command is adjusted continually by both human operator and feedback controller, which can cause unexpected conflict motions [11–15]. The feedforward techniques, on the other hand, modify the command before sending to the crane motors. The input shaping, a typical open-loop technique, is implemented by convolving a series of impulse, called the input shaper, with the reference command [11–15]. Although do not require the sensors, the input shaping cannot counteract disturbances or initial conditions due to its open-loop nature [16,17]. A recent comprehensive review of both feedback and feedforward control of crane can be found in Ref. [18].

The rather more conventional passive damping systems are introduced to control the payload swinging in some recent studies [19,20,21]. The radial spring-damper is a typical type of passive system can be used in anti-sway crane control [20,21]. It works in the principle of nonlinear Coriolis damping. The radial spring-damper is mounted in-line, between

* Corresponding author at: Institute of Mechanics, Vietnam Academy of Science and Technology, 264 Doi Can, Hanoi, Viet Nam.
E-mail address: ldviet@imech.vast.vn (V.D. La).

https://doi.org/10.1016/j.ymssp.2018.06.056
0888-3270/

the crane hook and the payload. Practically, the large payload weight should be the problem for introduction of additional mechanical device. However, in fact, some suppliers [22,23] supplied device called Passive Heave Compensation, which is the cylinder filled with gas, used to absorb shock in the crane's cable. This can be modeled as a combination of gas spring and gas damper. The problem of mechanical stress in spring can be avoided for this type of radial spring-damper.

In comparison with the feedback control, the passive approach has limited effectiveness. However, the passive system is simple in application and can be used as a secondary system to improve main control systems. Obviously, the technique does not rely on sensors should be the combination between the passive systems and the input shaping techniques.

The purpose of this paper is to introduce a combination of radial spring-damper with input shaping technique to control the tridirectional vibration of the crane payload induced by both human operators and initial conditions. Tridirectional vibration includes the vibration of tangential sway, radial sway and cable tension. The paper reveals that a single spring-damper system can simultaneously produce three dampings for those three vibrations. Each of three driving commands to a boom crane can be shaped for each of payload's degree of freedom. The paper includes two main parts. First, the effect of input shaping and radial spring-damper are clearly explained. Then the effectiveness of the combination is verified numerically and experimentally.

2. Problem statement

The concept of combination of input shaping and radial spring-damper to reduce the tridirectional vibration of a crane payload is shown in Fig. 1.

If the command from the crane operator is sent directly to the motor to move the crane, the oscillatory response is induced. Instead of that, the operator command is convolved with a series of impulses, called the input shaper, before sending to the motor. The general input shaper can be diagrammatized as shown in Fig. 2.

In Fig. 2, the gain blocks correspond to the impulse amplitudes, A_i while the time delay blocks correspond to the impulse time locations. In this paper, for the demonstration purpose, two simplest input shapers are considered: the zero vibration (ZV) shaper and the zero vibration and derivative (ZVD) shaper [13]. They are represented as:

$$ZV = \begin{bmatrix} A_i \\ \Delta_i \end{bmatrix} = \begin{bmatrix} 0.5 & 0.5 \\ 0 & \pi/\omega \end{bmatrix} \tag{1}$$

$$ZVD = \begin{bmatrix} A_i \\ \Delta_i \end{bmatrix} = \begin{bmatrix} 0.25 & 0.5 & 0.25 \\ 0 & \pi/\omega & 2\pi/\omega \end{bmatrix} \tag{2}$$

where ω is the natural frequency of the system modeled as a second order harmonic oscillator. A major advantage of the input shaping technique is that they do not require the sensors. However, they are lack the ability to handle external disturbances or initial conditions. In Ref. [20], a radial spring and damper is proposed to limit the free vibration induced by initial

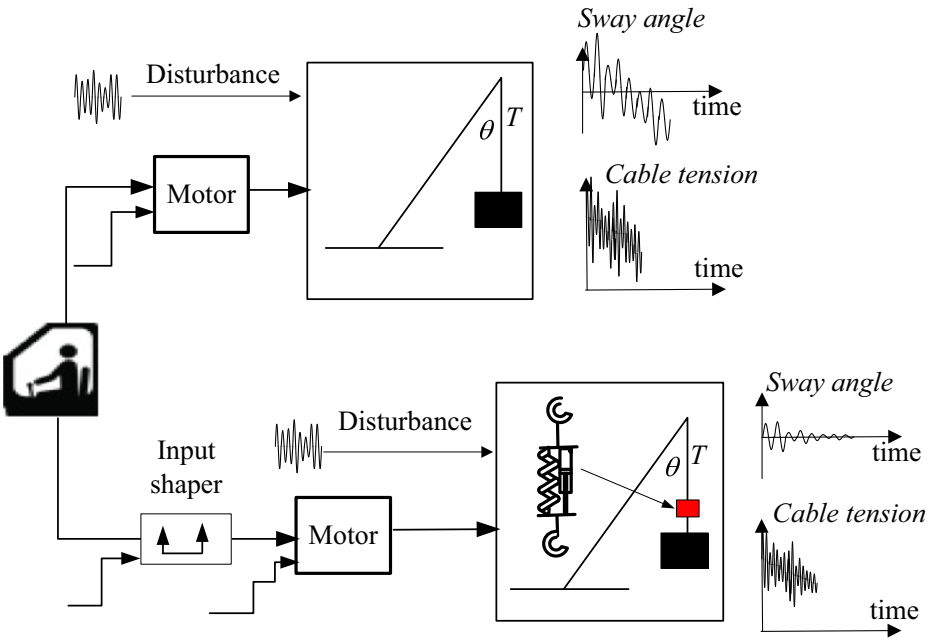

Fig. 1. Combination of input shaping and radial spring and damper.

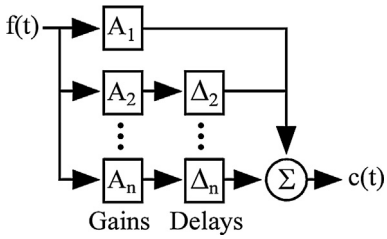

Fig. 2. Input Shaper represented by block diagram.

condition. In Ref. [21], the radial spring and damper can also reduce the sway angle induced by random disturbance. Moreover, because the spring-damper is mounted between the hook and the payload, it can partly prevent the payload's radial oscillation from transmitting to the cable, which reduces the fluctuation of the cable tension.

To clearly explain the mechanism of the spring and damper, consider the mathematical model of a boom crane attached with spring and damper as shown in Fig. 3.

The payload's sway motion induces the centrifugal force. The payload is connected to the hook through a spring-damper combination, which excites the payload's radial motion. The Coriolis damping produced by this radial motion acts on and reduces the payload's sway. Moreover, the damper also produces damping in radial direction to attenuate the fluctuation of the cable tension. In this way, a single damper can simultaneously produce three dampings in three directions.

To highlight the nature of each component in the combination approach, let's make the following assumptions:

- The payload's weight is large enough to ignore the spring-damper's weight.
- The cable's stiffness is large enough to ignore the cable's deformation.

Some symbols used in the model are shown in Fig. 3 and are explained in Table 1.

The position of the payload (x_P, y_P, z_P) is obtained as:

$$\begin{aligned} x_P &= -L_2 \sin\alpha\cos\beta - (L_3+u)(\sin\alpha\sin\theta_2 - \cos\alpha\sin\theta_1\cos\theta_2) \\ y_P &= L_2\cos\alpha\cos\beta + (L_3+u)(\cos\alpha\sin\theta_2 + \sin\alpha\sin\theta_1\cos\theta_2) \\ z_P &= L_1 + L_2\sin\beta - (L_3+u)\cos\theta_1\cos\theta_2 \end{aligned} \tag{3}$$

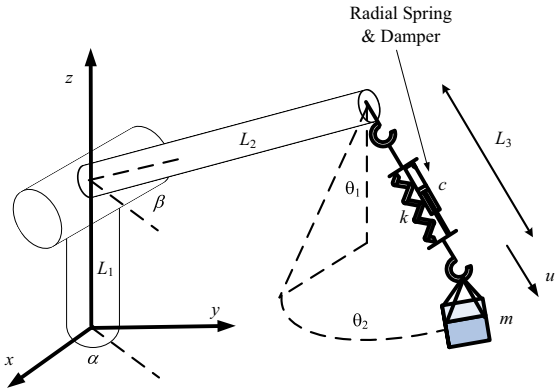

Fig. 3. Symbols used in the boom crane model.

Table 1
Description of symbols in Fig. 3.

Symbol	Description
m	Payload's mass
k, c	Spring and damper coefficients
θ_1, θ_2	Tangential pendulation and radial sway
L_1, L_2	Lengths of vertical column and boom
L_3	Hoist's length in static condition
α, β	Slew angle and luff angle
u	Radial motion measured from static position
g	Acceleration of gravity
M_1, M_2	Components of external (non-gravitational) moment vector

The dynamic model for this boom crane is derived by using Lagrange-Euler's method. After some manipulations, three Lagrange equations of motion reduce to:

$$\begin{aligned}&(L_3+u)(\ddot{\theta}_1\cos\theta_2-\ddot{\alpha}\cos\theta_1\sin\theta_2-2\dot{\theta}_2\dot{\alpha}\cos\theta_1\cos\theta_2-\dot{\alpha}^2\sin\theta_1\cos\theta_2\cos\theta_1-2\dot{\theta}_1\dot{\theta}_2\sin\theta_2)+2(\dot{L}_3+\dot{u})(\dot{\theta}_1\cos\theta_2\\&-\dot{\alpha}\cos\theta_1\sin\theta_2)-L_2\ddot{\alpha}\cos\theta_1\cos\beta-L_2\dot{\beta}^2\sin\beta\sin\theta_1+2L_2\dot{\alpha}\dot{\beta}\cos\theta_1\sin\beta+L_2\ddot{\beta}\cos\beta\sin\theta_1+g\sin\theta_1\\&=\frac{M_1}{m(L_3+u)\cos\theta_2}\end{aligned}\tag{4}$$

$$\begin{aligned}&(L_3+u)(\ddot{\theta}_2+2\dot{\theta}_1\dot{\alpha}\cos\theta_1\cos^2\theta_2+\ddot{\alpha}\sin\theta_1-\dot{\alpha}^2\cos\theta_2\sin\theta_2\cos^2\theta_1+\dot{\theta}_1^2\cos\theta_2\sin\theta_2)+2(\dot{L}_3+\dot{u})(\dot{\alpha}\sin\theta_1+\dot{\theta}_2)\\&-L_2\dot{\beta}^2\cos\beta\cos\theta_2-L_2\dot{\alpha}^2\cos\beta\cos\theta_2-L_2\dot{\beta}^2\sin\beta\cos\theta_1\sin\theta_2+g\cos\theta_1\sin\theta_2+L_2\ddot{\beta}\cos\beta\cos\theta_1\sin\theta_2\\&-2L_2\dot{\alpha}\dot{\beta}\sin\beta\sin\theta_1\sin\theta_2-L_2\ddot{\beta}\sin\beta\cos\theta_2+L_2\ddot{\alpha}\cos\beta\sin\theta_1\sin\theta_2=\frac{M_2}{m(L_3+u)}\end{aligned}\tag{5}$$

$$\begin{aligned}&\ddot{u}+\frac{k}{m}u+\frac{c}{m}\dot{u}+(L_3+u)\begin{pmatrix}\dot{\alpha}^2\cos^2\theta_2\cos^2\theta_1-\dot{\theta}_2^2-2\dot{\alpha}\dot{\theta}_2\sin\theta_1\\-\dot{\alpha}^2+2\dot{\alpha}\dot{\theta}_1\sin\theta_2\cos\theta_1\cos\theta_2-\dot{\theta}_1^2\cos^2\theta_2\end{pmatrix}\\&-L_2(\dot{\alpha}^2+\dot{\beta}^2)\cos\beta\sin\theta_2-L_2\ddot{\alpha}\cos\beta\sin\theta_1\cos\theta_2-L_2\ddot{\beta}\cos\beta\cos\theta_1\cos\theta_2\\&+L_2\dot{\beta}^2\sin\beta\cos\theta_1\cos\theta_2+\ddot{L}_3-L_2\ddot{\beta}\sin\beta\sin\theta_2+2L_2\dot{\alpha}\dot{\beta}\sin\beta\sin\theta_1\cos\theta_2+g(1-\cos\theta_1\cos\theta_2)=0\end{aligned}\tag{6}$$

One can see that the equation of motion describing tridirectional motion of the payload is nonlinear and complex. The simplified dynamic of boom crane model is obtained by assuming the small velocities and accelerations of slew, luff angles and hosting length, small angles, velocities and accelerations of sway, small displacements, velocities and accelerations of radial motion. Retaining the first order of $\ddot{\theta}_1,\dot{\theta}_1,\theta_1,\ddot{\theta}_2,\dot{\theta}_2,\theta_2,\ddot{\alpha},\dot{\alpha},\ddot{\beta},\dot{\beta},\ddot{L}_3,\dot{L}_3,\ddot{u},\dot{u},u$ simplifies (4), (5) and (6) to:

$$L_3\ddot{\theta}_1-L_2\ddot{\alpha}\cos\beta+g\theta_1=\frac{M_1}{mL_3}\tag{7}$$

$$L_3\ddot{\theta}_2+g\theta_2-L_2\ddot{\beta}\sin\beta=\frac{M_2}{mL_3}\tag{8}$$

$$\ddot{u}+\frac{k}{m}u+\frac{c}{m}\dot{u}-L_2\ddot{\beta}\cos\beta+\ddot{L}_3=0\tag{9}$$

The linearized Eqs. (7) and (8) show that the accelerations of slew and luff angles drive the sway angles. That means the input shaping can be applied to the slew and luff signals, using the natural frequency of the pendulum. The remaining Eq. (9) indicates that the radial motion is affected by the accelerations of luff angle and hoisting length. Therefore, the input shaping can be applied to the hoisting signal, using the natural frequency of the mass-spring system. Moreover, in the first order, there is only the presence of radial damping but not sway damping. That means the sway damping is indeed nonlinear [20,21].

Consider the case that the crane is in rest position $\ddot{\alpha}=\dot{\alpha}=\ddot{\beta}=\dot{\beta}=\ddot{L}_3=\dot{L}_3=0$. To the second order of $\ddot{\theta}_1,\dot{\theta}_1,\theta_1,\ddot{\theta}_2,\dot{\theta}_2,\theta_2,\ddot{u},\dot{u},u$, Eqs. (4), (5) and (6) reduce to:

$$\left(L_3^2+2L_3u\right)\ddot{\theta}_1+2L_3\dot{u}\dot{\theta}_1+(L_3+u)g\theta_1=\frac{M_1}{m}\tag{10}$$

$$\left(L_3^2+2L_3u\right)\ddot{\theta}_2+2L_3\dot{u}\dot{\theta}_2+(L_3+u)g\theta_2=\frac{M_2}{m}\tag{11}$$

$$\ddot{u}+\frac{k}{m}u+\frac{c}{m}\dot{u}-L_3\left(\dot{\theta}_2^2+\dot{\theta}_1^2\right)+\frac{g}{2}\left(\theta_1^2+\theta_2^2\right)=0\tag{12}$$

These equation was studied in Ref. [21], where the terms $2L_3\dot{u}\dot{\theta}_1$ and $2L_3\dot{u}\dot{\theta}_2$ produce the Coriolis dampings to reduce the sway motion. The results in Ref. [21] indicate that the frequency ratio between the mass-spring system and the pendulum should be near 2, i.e.:

$$r=\sqrt{\frac{k}{m}}\Big/\sqrt{\frac{g}{L_3}}\approx 2\tag{13}$$

where r is the frequency ratio. Moreover, the relations between three damping ratios are also presented [21]:

$$\zeta_i=\frac{S_i}{m^2L_3^4\omega^3}\,\frac{2r^4\zeta_i+8\zeta r^2\zeta_i^2+8\zeta_i^3r^2-3r^2\zeta_i+3\zeta r^2+4\zeta_i+16\zeta^2\zeta_i+16\zeta_i^2\zeta}{\left(r^2+4\zeta_i^2+4\zeta\zeta_i\right)\left(\left(r^2-4\right)^2+16r^2\zeta_i^2+8r^2\zeta_i\zeta+16\zeta^2+32\zeta\zeta_i\right)\zeta_i}\,(i=1,2)\tag{14}$$

where S_i ($i = 1, 2$) are the intensities of the white noise moments M_i ($i = 1, 2$), ζ_i ($i = 1, 2$) are two sway damping ratios, ζ is radial damping ratio determined as:

$$\zeta = \frac{c}{2m\omega} \tag{15}$$

where ω is the natural frequency of pendulum. The formulas (14) also show the following relation between the dampings. If the radial damping is too large ($\zeta = \infty$) or too small ($\zeta = 0$) then the sway dampings (Coriolis dampings) ζ_i ($i = 1, 2$) tend to zeros.

3. Numerical demonstration

In order to demonstrate the effectiveness of the combination approach, a boom crane model is simulated independently using the software RECURDYN [24]. The model's parameters are taken from [25] as follows: $L_1 = 0.627$ m, $L_2 = 0.845$ m, $m = 1.5$ kg. The crane model in RECURDYN is shown in Fig. 4.

The spring is chosen such that r (defined in Eq. (13)) is equal to 2. The damper is chosen such that ζ (defined in Eq. (15)) is equal to 60%. The velocity commands are also taken from [25] and shown in Fig. 5.

The complex motion is defined as follows:

- In the first period from 0 to 3.5 s, the slewing base rotates from the position $\alpha = 0$, the boom rotates in vertical plane from the position $\beta = 30°$, the hoisting length increases from the position $L_3 = 0.9$ m
- In the second period from 3.5 s to 7 s, the slewing base continues rotating to the position $\alpha = 90°$, the boom rotates from the position $\beta = 50°$ to the initial luff angle, the hoisting length decreases to the initial length.

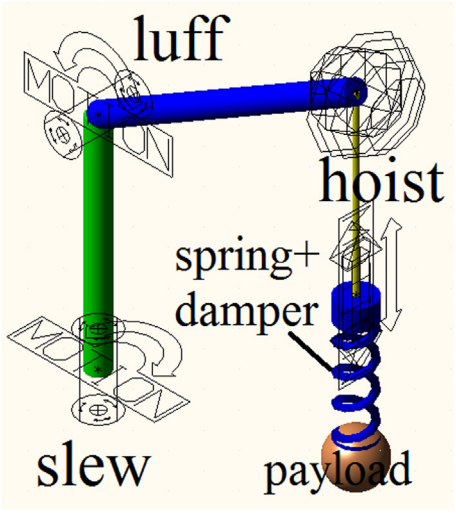

Fig. 4. Crane model in RECURDYN.

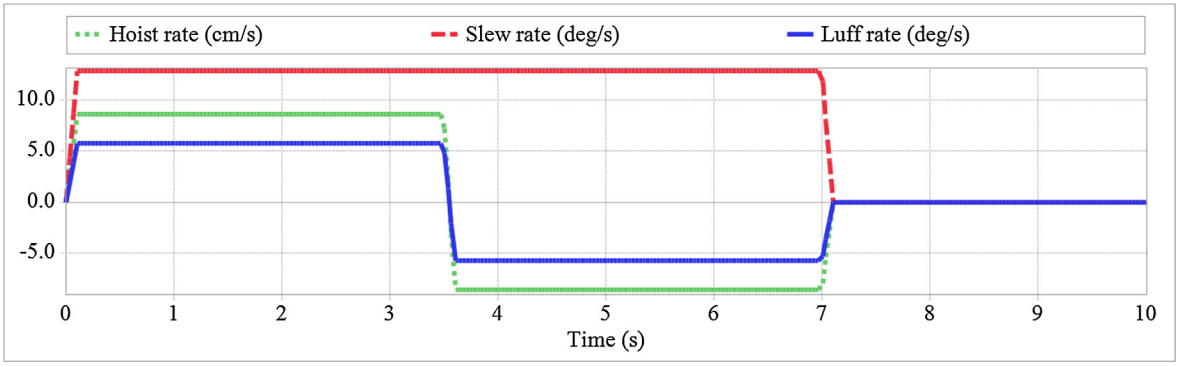

Fig. 5. Commanded velocities.

The ZV input shaper (1) is applied to three commands using the natural frequencies in the linearized model (7), (8) and (9). The initial length is used to determine the frequency. It is noted that the parameters of the input shaping and spring-damper are determined from the case of constant pendulum length. The numerical simulation of varying hoisting length, therefore, also checks the robustness of the parameters chosen. The shaped commands are shown in Fig. 6.

The disturbance is demonstrated by the payload's initial velocity. This type of initial condition can be the result of a short and large wind gust. For demonstration, we take the initial velocity as a three-component vector = [1,1,0] m/s. The effectiveness in reducing tridirectional vibration is evaluated by two indexes: the cable tension and the sway angle (measured from the vertical). The comparisons are shown in Figs. 7–10.

Some following remarks can be drawn:

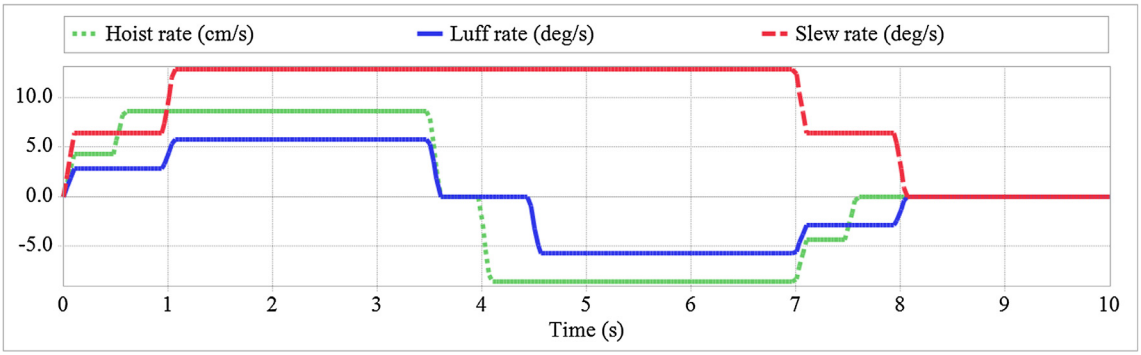

Fig. 6. Shaped velocity profiles.

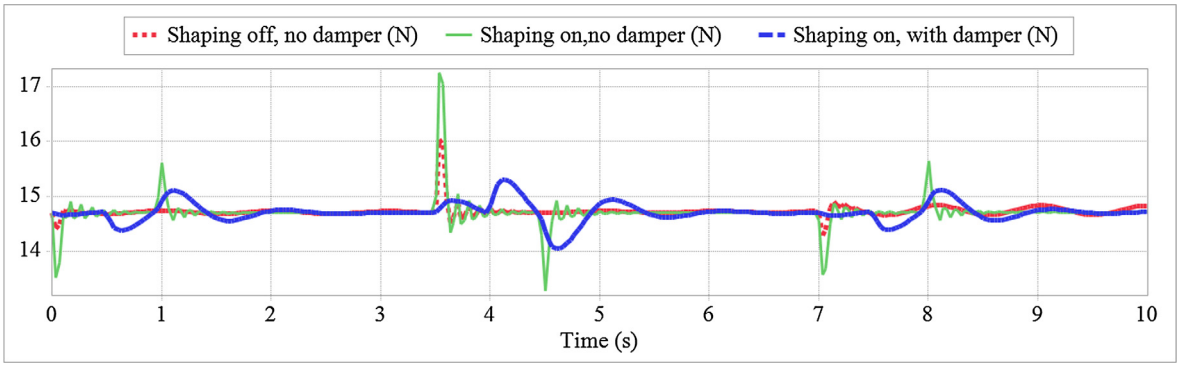

Fig. 7. Cable tension resulting from crane motion.

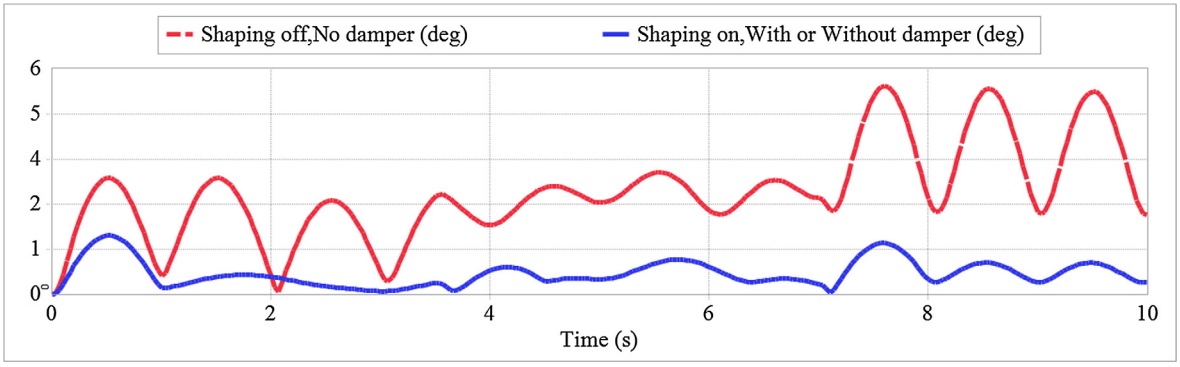

Fig. 8. Sway angle resulting from crane motion.

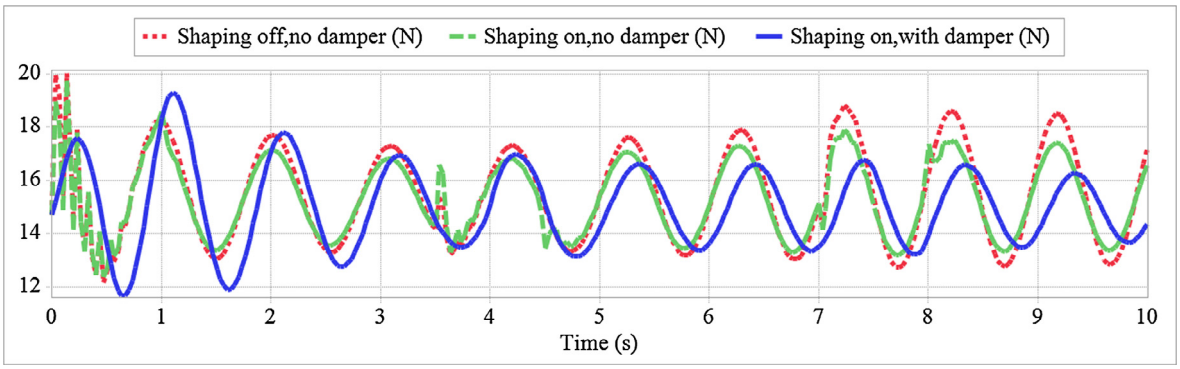

Fig. 9. Cable tension resulting from crane motion and gust disturbance.

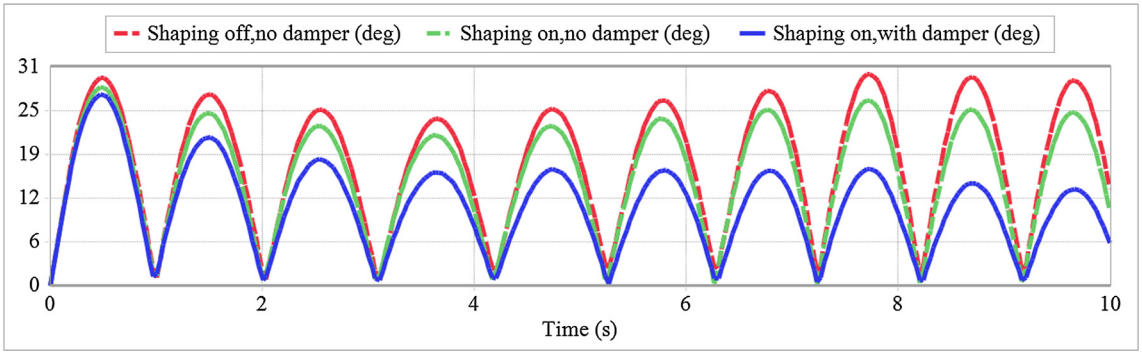

Fig. 10. Sway angle resulting from crane motion and gust disturbance.

- Without disturbance, the damper's effect in reducing the sway angle is not clear (Fig. 8). The reason is that the input shaping significantly suppresses the deflection to the linear region, in which the damper has little effect. However the change of the cable tension is smoother thanks to the damper (Fig. 7).
- With disturbance, the input shaping cannot deal with the disturbance but the damper can attenuate the induced vibration (Figs. 9 and 10).
- The radial damper only shows effect for the large sway. For a small sway, the radial damper is not good but does not worsen the performance (Fig. 8). If the practical target is to keep the sway below a certain level, the radial damper can have its practical advantage.
- In any case, the combination proposed shows its good effectiveness. This is due to the combined advantages of two components.

4. Experimental verification

A simple experiment is set up to demonstrate the effectiveness of the proposed approach. Fig. 11a–b presents the setups used.

In Fig. 11a, the experimental model has a 0.846 m boom's length and 1 kg payload. A digital camera is mounted at the tip of the boom through a four-bar mechanism and records the swing deflection of the payload. The payload is painted black for image processing. The spring-damper mechanism is shown in Fig. 11b. Some magnets are used to provide the magnetic damping of the mechanism. The natural frequency of the pendulum is about 3.88 rad/s while the natural frequency of the mass-spring system is about 10.1 rad/s. The spring is not truly optimized as desired (see Eq. (13)). The optimized spring should be softer, which requires some special treatments to limit the static deflection. For example, the preload spring or gas spring can be used. In this experiment, although the simple spring is not optimized, some attenuation effects are still observed. The magnetic damping is about 13%.

The sway motion induced by initial angle is shown in Figs. 12–15 in both horizontal and vertical planes. The vertical motion induced by initial vertical displacement is also shown in Fig. 16. It is noted that when the crane does not move, the input shaping technique (and any other control schemes based on the crane motion) cannot be used. Therefore, in Figs. 12–15, only two cases of with and without damper are compared.

Fig. 11. Boom crane (a) and spring-damper mechanism (b).

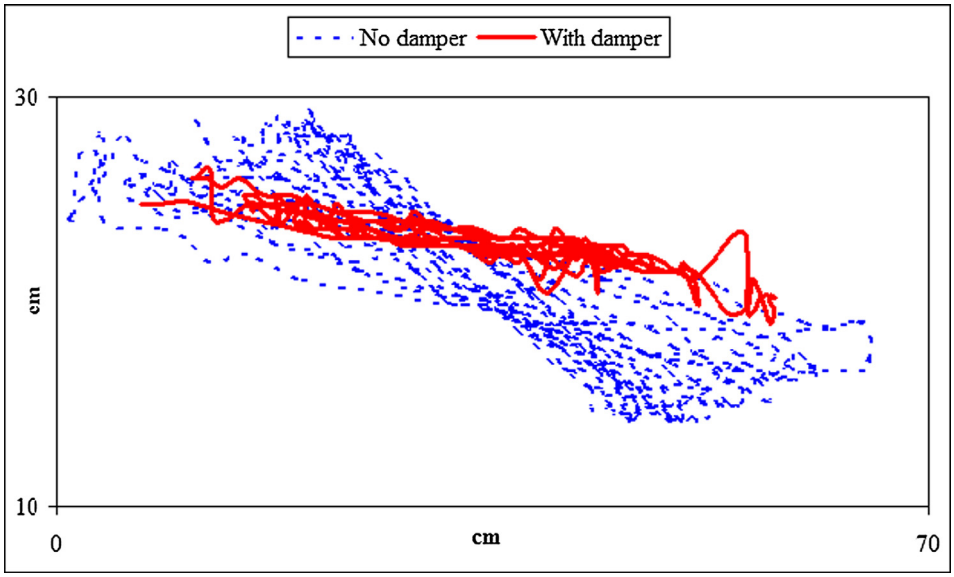

Fig. 12. Payload's orbit in horizontal plane, free vibration.

The results show that the radial spring-damper can produce damping in both horizontal plane (Fig. 13) and vertical direction (Fig. 16). As explained in Section 2, this single damper can simultaneously produce three dampings in three directions.

The effect of the combination of input shaping and radial spring-damper can also be seen by rotating the crane base. A trapezoidal-velocity profile (bang-coast-bang acceleration) is used to drive the crane. The slewing velocity rises to 2 rad/s in 0.1 s. Then the base rotates at this velocity in 3 s. Then the velocity decreases to zero in 0.1 s. The ZVD shaper (2) is used for demonstration. The comparisons of orbits in horizontal plane and deflections in two horizontal directions are shown in Figs. 17–19. The comparison of sway angle (measured from vertical) is plotted in Fig. 20.

One can see that the input shaping can significantly reduce the sway motion while the radial spring-damper makes some more improvements. As seen in Fig. 20, when the sway angle is still large (before 12 s), apart from the reduction given by the input shaping, the spring-damper adds some more reduction to the sway angle. After 12 s, the sway angle is quite small that the damper also has little effect. After 12 s, with damper, the X-deflection is even higher than that of without damper (Fig. 18). However, the sway angle in Fig. 20 shows that the difference is very small. The practical advantage of the damper

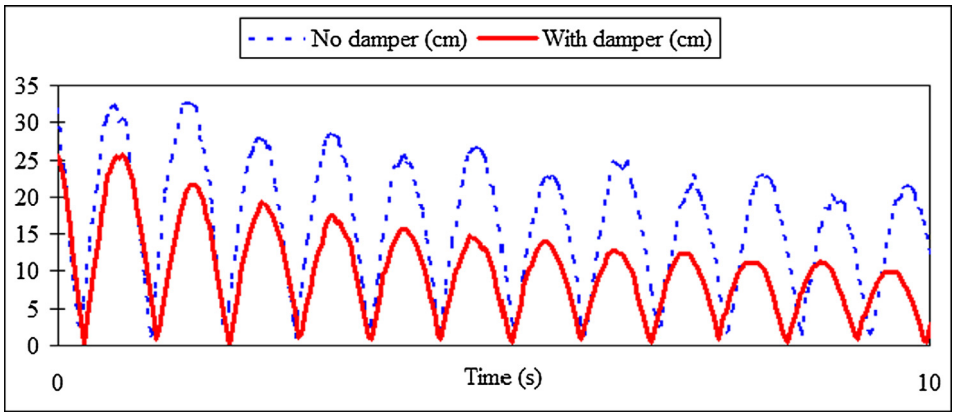

Fig. 13. Payload's deflection in horizontal plane, free vibration.

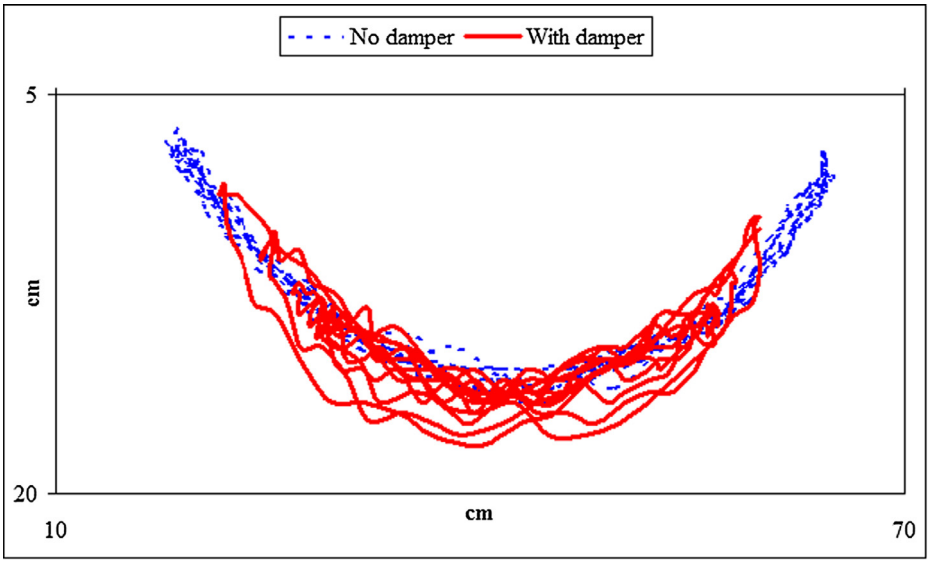

Fig. 14. Payload's orbit in vertical plane, free vibration.

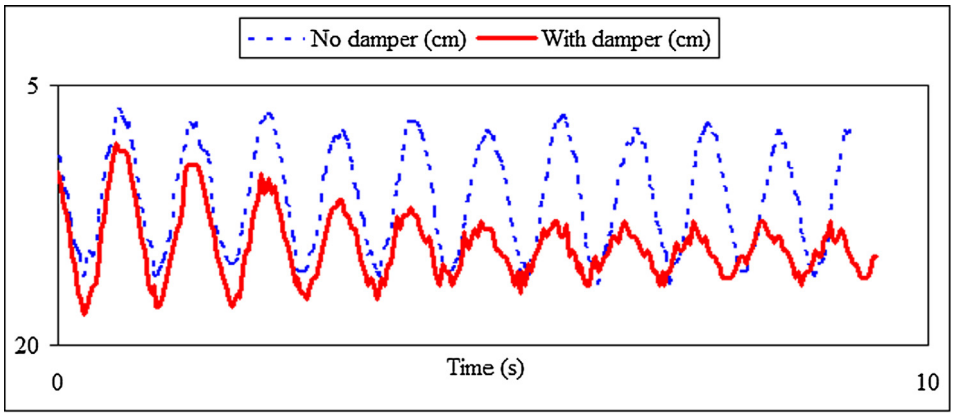

Fig. 15. Payload's height, free vibration.

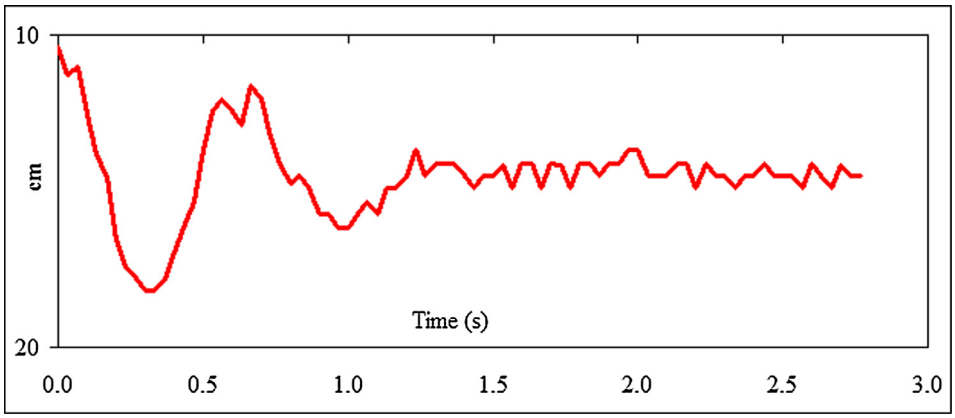

Fig. 16. Vertical motion of payload induced by initial vertical displacement.

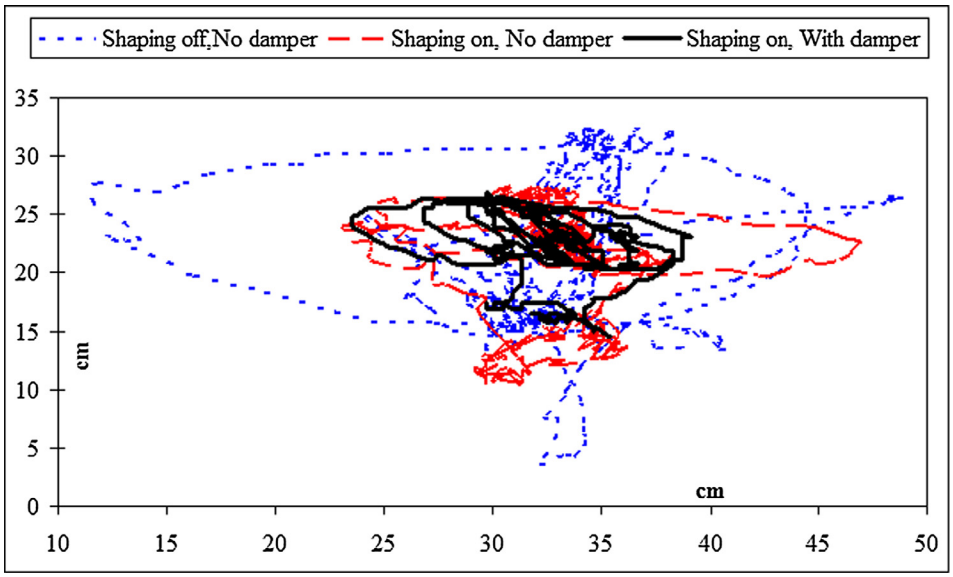

Fig. 17. Payload's orbit in horizontal plane, sway induced by slewing.

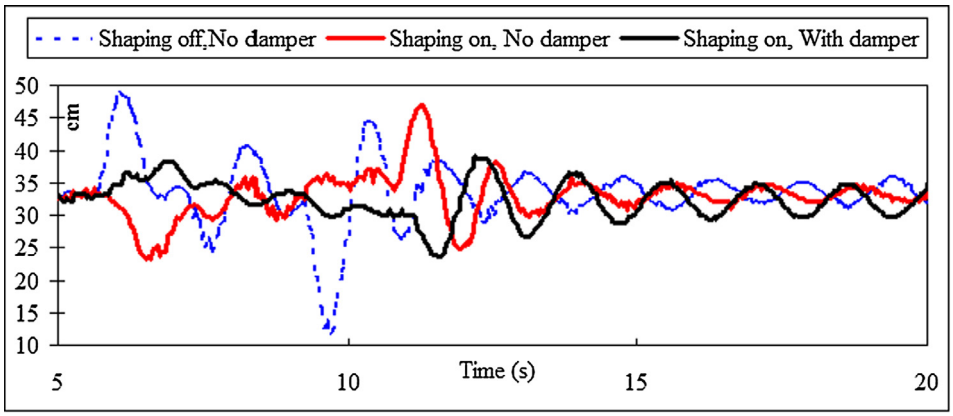

Fig. 18. Horizontal X deflection, sway induced by slewing.

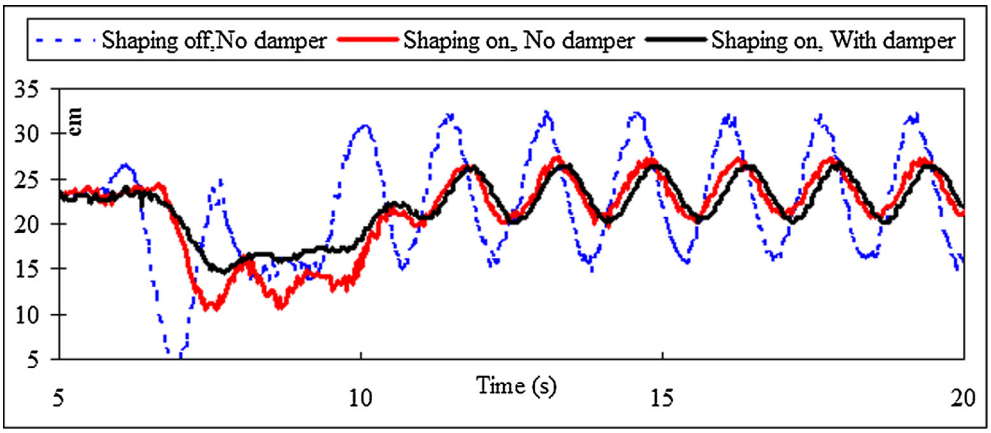

Fig. 19. Horizontal Y deflection, sway induced by slewing.

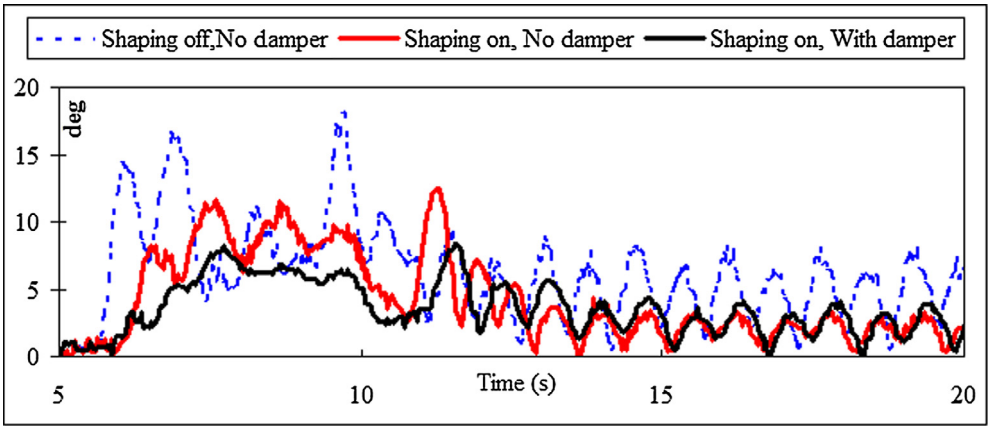

Fig. 20. Sway angle induced by slewing.

is: the damper does not worsen the small sway (after 12 s) but significantly reduce the large sway (before 12 s). The experiment's results verify that the combination approach can reduce the payload's sway induced by both human operators and initial conditions.

5. Conclusions

The novelty of this paper is to propose and analysis of the combination between two sensorless approaches to reduce the tridirectional vibration of a crane payload. The first approach uses the input shaper to reduce the motion induced by operator. The second approach uses a radial spring-damper to produce three dimensional damping. The numerical and experimental analyses show that the proposed combination can effectively reduce the oscillatory responses induced by both initial condition and human operator.

Acknowledgement

This research is funded by Vietnam National Foundation for Science and Technology Development (NAFOSTED) under grant number "107.01-2015.35".

References

[1] Dongho Kim, Youngjin Park, Tracking control in x-y plane of an offshore container crane, J. Vib. Control (2015), https://doi.org/10.1177/1077546315581091.
[2] D.H. Kim, J.W. Lee, Model-based PID control of a crane spreader by four auxiliary cables, Proc. Inst. Mech. Eng. Part C: J. Mech. Eng, Sci. 220 (2006) 1151–1165.
[3] Z. Masoud, Oscillation control of quay-side container cranes using cable-length manipulation, J. Dyn. Syst. Meas. Contr. 129 (2007) 224–228.

[4] H.H. Lee, Y. Liang, D. Segura, A sliding-mode antiswing trajectory control for overhead cranes with high-speed load hoisting, J. Dyn. Syst. Meas. Contr. 128 (2006) 842–845.
[5] J. Neupert, E. Arnold, K. Schneider, O. Sawodny, Tracking and anti-sway control for boom cranes, Control Eng. Pract. 18 (2010) 31–44.
[6] N. Uchiyama, Robust control of rotary crane by partial-state feedback with integrator, Mechatronics 19 (2009) 1294–1302.
[7] H. Kawai, Y.B. Kim, Y.W. Choi, Anti-sway system with image sensor for container cranes, J. Mech. Sci. Technol. 23 (2009) 2757–2765.
[8] Jaroslaw Smoczek, Fuzzy crane control with sensorless payload deflection feedback for vibration reduction, Mech. Syst. Sig. Process. 46 (2014) 70–81.
[9] Menghua Zhang, Xin Ma, Xuewen Rong, Xincheng Tian, Yibin Li, Adaptive tracking control for double-pendulum overhead cranes subject to tracking error limitation, parametric uncertainties and external disturbances, Mech. Syst. Sig. Process. 76–77 (2016) 15–32.
[10] M. Böck, A. Kugi, Real-time nonlinear model predictive path-following control of a laboratory tower crane, IEEE Trans. Control Syst. Technol. 22 (4) (2014) 1461–1473.
[11] J. Vaughan, E. Maleki, W. Singhose, Advantages of using command shaping over feedback for crane control, in: Proc. of American Control Conference, Baltimore, USA, 2010, pp. 2308–2313.
[12] J. Lawrence, W. Singhose, Command shaping slewing motions for tower cranes, J. Vib. Acoust. 132 (2010) 011002.
[13] J. Vaughan, A. Yano, W. Singhose, Comparison of robust input shapers, J. Sound Vib. 315 (2008) 797–815.
[14] D. Blackburn, W. Singhose, J. Kitchen, V. Patrangenaru, J. Lawrence, Tatsuaki Kamoi, Ayako Taura, Command shaping for nonlinear crane dynamics, J. Vib. Control 16 (2010) 1–25.
[15] William Singhose, Command shaping for flexible systems: a review of the first 50 years, Int. J. Precis. Eng. Manuf. 10 (4) (2009) 153–168.
[16] Jie Huang, Ehsan Maleki, William Singhose, Dynamics and swing control of mobile boom cranes subject to wind disturbances, IET Control Theory Appl. 7 (9) (2013) 1187–1195.
[17] Robert Schmidt, Nicole Barry, Joshua Vaughan, Tracking of a target payload via a combination of input shaping and feedback control, IFAC-PapersOnLine 48 (12) (2015) 141–146.
[18] Liyana Ramli, Z. Mohamed, Auwalu M. Abdullahi, H.I. Jaafar, Izzuddin M. Lazim, Control strategies for crane systems: a comprehensive review, Mech. Syst. Sig. Process. 95 (2017) 1–23.
[19] La Duc Viet, Youngjin Park, A cable-passive damper system for sway and skew motion control of a crane spreader, Shock Vib. 2015 (2015) 507549.
[20] L.D. Viet, Crane sway reduction using Coriolis force produced by radial spring and damper, J. Mech. Sci. Technol. 29 (3) (2015) 973–979.
[21] Viet Duc La, Partial stochastic linearization of a spherical pendulum with Coriolis damping produced by radial spring and damper, J. Vib. Acoust 137 (5) (2015) 054504.
[22] Cranemaster, http://www.cranemaster.com, last checked 27 May 2018.
[23] Safelink, http://www.safelink.no, last checked 27 May 2018.
[24] Function Bay Inc., http://www.functionbay.co.kr/, last checked 27 May 2018.
[25] Kazuhiko Terashima, Ying Shen, Ken'ichi Yano, Modeling and optimal control of a rotary crane using the straight transfer transformation method, Control Eng. Pract. 15 (2007) 1179–1192.